

Dihydrophenanthrene-Based Metal-Free Dyes for Highly Efficient Cosensitized Solar Cells

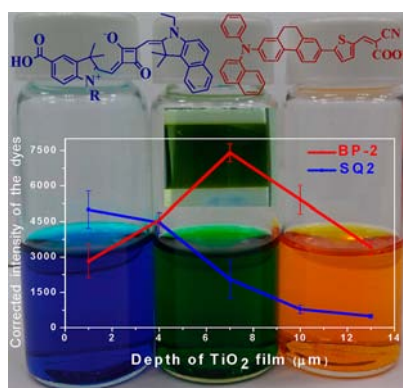
Ryan Yeh-Yung Lin,^{†,‡} Yung-Sheng Yen,[†] Yung-Tse Cheng,^{†,§} Chuan-Pei Lee,[‡] Ying-Chan Hsu,[†] Hsien-Hsin Chou,[†] Chih-Yu Hsu,[†] Yung-Chung Chen,[†] Jiann T. Lin,^{*,†} Kuo-Chuan Ho,^{*,‡,||} and Chiitang Tsai[§]

Institute of Chemistry, Academia Sinica, Nankang, Taipei 11529, Taiwan, Department of Chemical Engineering, National Taiwan University, Taipei, 10617, Taiwan, Department of Chemistry, Chinese Culture University, Taipei, Taiwan, and Institute of Polymer Science and Engineering, National Taiwan University, Taipei 10617, Taiwan

jtlin@gate.sinica.edu.tw; kcho@ntu.edu.tw

Received May 18, 2012

ABSTRACT



Metal-free dyes (BP-1 to BP-3) containing a 9,10-dihydrophenanthrene unit in the spacer have been synthesized. The dye with the highest cell efficiency, BP-2, was used in combination with SQ2 for cosensitized DSSCs. The cosensitized DSSC in which the ratio of BP-2 and SQ2 is 8:2 (v/v) has a record high efficiency of 8.14% among cosensitized systems using all metal-free sensitizers. Dye distribution along the TiO₂ film depth was analyzed by an Auger electron spectroscopy technique.

Searching for clean and sustainable energy is one of the most important scientific and technological challenges in the 21st century. Compared to other renewable energy resources, solar energy is very attractive because of its unlimited supply. Dye-sensitized solar cells (DSSCs) based

on organic materials have received considerable attention in the past two decades. DSSCs based on Ru complexes have achieved efficiencies of > 11% at standard AM 1.5G irradiation.¹ The best efficiency of metal-free sensitizer-based DSSCs reaches only ~10%.² Nonetheless, metal-free dyes are very attractive in view of some disadvantages of Ru sensitizers: (1) Ru metal is expensive and less environmentally friendly; (2) the metal-to-ligand charge-transfer

[†] Academia Sinica.

[‡] Department of Chemical Engineering, National Taiwan University.

[§] Chinese Culture University.

^{||} Institute of Polymer Science and Engineering, National Taiwan University.

(1) (a) Nazeeruddin, M. K.; Péchy, P.; Renouard, T.; Zakeeruddin, S. M.; Humphry-Baker, R.; Comte, P.; Liska, P.; Cevey, L.; Costa, E.; Shklover, V.; Spiccia, L.; Deacon, G. B.; Bignozzi, C. A.; Grätzel, M. *J. Am. Chem. Soc.* **2001**, *123*, 1613. (b) Nazeeruddin, M. K.; De Angelis, F.; Fantacci, S.; Selloni, A.; Viscardi, G.; Liska, P.; Ito, S.; Bessho, T.; Grätzel, M. *J. Am. Chem. Soc.* **2005**, *127*, 16835.

(2) (a) Zeng, W.; Cao, Y.; Bai, Y.; Wang, Y.; Shi, Y.; Zhang, M.; Wang, F.; Pan, C.; Wang, P. *Chem. Mater.* **2010**, *22*, 1915. (b) Mishra, A.; Fischer, M. K. R.; Bäuerle, P. *Angew. Chem., Int. Ed.* **2009**, *48*, 2474. (c) Hagfeldt, A.; Boschloo, G.; Sun, L.; Kloo, L.; Pettersson, H. *Chem. Rev.* **2010**, *110*, 6595. (d) Yen, Y.-S.; Chou, H.-H.; Chen, Y.-C.; Hsu, C.-Y.; Lin, J. T. *J. Mater. Chem.* **2012**, *22*, 8734.

(MLCT) band of the Ru dye normally does not have molar extinction coefficients $>25\,000\text{ M}^{-1}\text{ cm}^{-1}$ and a thicker TiO_2 film is needed.

A small molecule sensitizer normally does not have a broad absorption covering most of the visible to near-infrared (NIR) region of the solar spectrum. In order for a DSSC to have panchromatic absorption, use of different sensitizers absorbing in different regions of the solar spectrum appears to be a convenient approach because the short-circuit current density (J_{SC}) and thus the conversion efficiency (η) can be improved. Cosensitized DSSCs thus received increasing attention in recent years, and significant progress has been made.^{3a} Cosensitizing systems using a metal-free dye and a ruthenium dye have been proved to be successful since the former has intense absorption at shorter wavelengths and the latter absorbs at longer wavelengths extending into the red to NIR region. For example, Ogura et al. used the black dye in combination with D131, and the efficiency was increased by $\sim 1\%$ compared to the cell with the black dye only.^{3b} Ko et al. reported that the cosensitized DSSC based on a ruthenium sensitizer (JK-142) and a metal-free dye (JK-62) exhibited an efficiency (10.2%) surpassing that using only a single sensitizer (JK-142, 7.28%; JK-62, 5.36%).^{3c} More recently Han et al. also reported a very high efficiency (11.4%) cosensitized DSSC using a metal-free dye and the black dye.^{3d} A DSSC with record high performance (12.3%) was demonstrated with the use of two metal-containing porphyrin dyes as cosensitizers together with the use of a Co(II/III)-based redox electrolyte.^{3e} Diau et al. and Kimura et al. independently reported cosensitized systems of porphyrin with organic dyes exhibited improved performance in 2012.^{3f,g} In comparison, there were also successful examples of cosensitized DSSCs using solely metal-free dyes. Nazeeruddin et al. and Torres et al. employed NIR dyes (SQ1 or TT1) together with the JK2 for the cosensitized solar cell.^{3h,i} The action spectra (IPCE) could extend up to 700 nm, and the device efficiency over 7% was achieved. Choi et al. achieved a high performance (8.65%) cosensitized solar cell using JK2 and SQ1 dyes and

Al_2O_3 -coated TiO_2 to retard the electron recombination rate.^{3j} An interesting ultrafast cosensitization was reported by Holliman et al., with the best efficiency of 7.2%.^{3k}

Previously we developed thienylfluorene-based dyes with high light-harvesting efficiencies.⁴ One of the dyes, (*E*)-2-cyano-3-(5-(9,9-diethyl-7-(naphthalen-1-yl)(phenyl)-amino)-9*H*-fluoren-2-yl)thiophen-2-yl)acrylic acid (**FL** dye), was used as a cosensitizer of either N719 dye or black dye with improved cell performance.⁵ We also tested the combination of the **FL** dye with an NIR-absorbing squaraine dye, SQ2.⁶ However, the performance of cosensitized DSSC was inferior to that of DSSCs based on either **FL** or SQ2. Since a slight change of molecular conformation may have a significant impact on the cell performance,⁷ we set out to develop congeners of the **FL** dye in which the fluorene entity is replaced by a 9,10-dihydrophenanthrene entity based on two reasons: (1) the skeleton of 9,10-dihydrophenanthrene is similar to that of fluorene, and the good light-harvesting character of the **FL** dye can be retained; (2) a slight change of the dye conformation may lead to better dye packing of the cosensitizers. A series of 9,10-dihydrophenanthrene-based sensitizers (**BP-1** to **BP-3**) (Figure 1) were thus synthesized, and the synthetic protocols are shown in Scheme S1 (see Supporting Information (SI)).

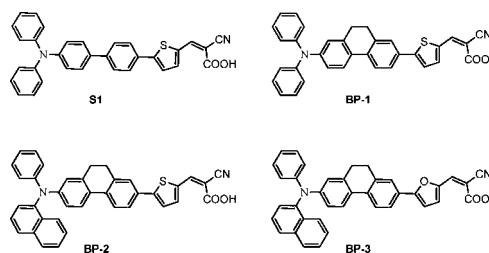


Figure 1. Structures of the dyes.

All of the **BP** dyes exhibit two prominent bands in the absorption spectra (Figure 2), the one at a longer wavelength region (410–500 nm) and with a high molar absorption coefficient ($\epsilon > 36\,500\text{ M}^{-1}\text{ cm}^{-1}$) is attributed to π – π^* transition with charge transfer character. The λ_{abs}

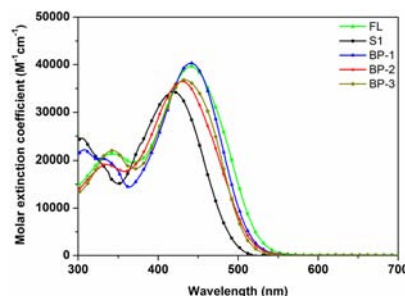


Figure 2. Absorption spectra of the dyes in THF.

(3) (a) Yum, J.-H.; Baranoff, E.; Wenger, S.; Nazeeruddin, M. K.; Grätzel, M. *Energy Environ. Sci.* **2011**, *4*, 842. (b) Ogura, R.-Y.; Nakane, S.; Morooka, M.; Orihashi, M.; Suzuki, Y.; Noda, K. *Appl. Phys. Lett.* **2009**, *94*, 073308. (c) Fan, S.-Q.; Kim, C.; Fang, B.; Liao, K.-X.; Yang, G.-J.; Li, C.-J.; Kim, J.-J.; Ko, J. *J. Phys. Chem. C* **2011**, *115*, 7747. (d) Han, L.; Islam, A.; Chen, H.; Malapaka, C.; Chiranjeevi, B.; Zhang, S.; Yang, X.; Yanagida, M. *Energy Environ. Sci.* **2012**, *5*, 6057. (e) Yella, A.; Lee, H.-W.; Tsao, H. N.; Yi, C.; Chandiran, A. K.; Nazeeruddin, M. K.; Diau, E. W.-G.; Yeh, C.-Y.; Zakeeruddin, S. M.; Grätzel, M. *Science* **2011**, *334*, 629. (f) Lan, C.-M.; Wu, H.-P.; Pan, T.-Y.; Chang, C.-W.; Chao, W.-S.; Chen, C.-T.; Wang, C.-L.; Lin, C.-Y.; Diau, E. W.-G. *Energy Environ. Sci.* **2012**, *5*, 6460. (g) Kimura, M.; Nomoto, H.; Masaki, N.; Mori, S. *Angew. Chem., Int. Ed.* **2012**, *51*, 4371. (h) Cid, J. J.; Yum, J. H.; Jang, S. R.; Nazeeruddin, M. K.; Martinez-Ferrero, E.; Palomares, E.; Ko, J.; Grätzel, M.; Torres, T. *Angew. Chem., Int. Ed.* **2007**, *46*, 8358. (i) Yum, J.-H.; Jang, S.-R.; Walter, P.; Geiger, T.; Nüesch, F.; Kim, S.; Ko, J.; Grätzel, M.; Nazeeruddin, M. K. *Chem. Commun.* **2007**, 4680. (j) Choi, H.; Kim, S.; Kang, S. O.; Ko, J.; Kang, M.-S.; Clifford, J. N.; Forneli, A.; Palomares, E.; Nazeeruddin, M. K.; Grätzel, M. *Angew. Chem., Int. Ed.* **2008**, *47*, 8259. (k) Holliman, P. J.; Mohsen, M.; Connell, A.; Davies, M. L.; Al-Salihi, K.; Pitak, M. B.; Tizzard, G. J.; Coles, S. J.; Harrington, R. W.; Clegg, W.; Serpa, C.; Fontes, O. H.; Charbonneau, C.; Carnie, M. *J. Mater. Chem.* **2012**, *22*, 13318.

decreases in the order of **FL** (443 nm) > **BP-2** (430 nm) and **BP-1** (441 nm) > **S1** (418 nm), which is in accordance with the degree of planarity of the two phenyl rings in the conjugated spacer (vide infra). Blue-shifted absorption spectra of the dyes on TiO₂ (Figure S1) is attributed to the deprotonation of the carboxylic acid. The cyclic voltammograms of the dyes are shown in Figure S2 (SI). The more planar configuration of the **BP** dye than **S1** allows better electronic communication between the arylamine and electron excessive heteroaromatic ring; consequently the former displays a negatively shifted oxidation wave (Table 1). Quantum chemistry computation was carried out, and the results for the theoretical approach are included in Table S1 (SI). Frontier orbitals, Mulliken charge shifts, the corresponding energy states, and optimized molecular conformation are shown in Figures S3–S6 (SI), respectively.

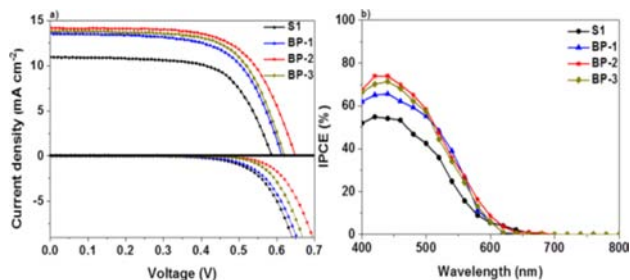


Figure 3. (a) J - V curves and (b) IPCE spectra of DSSCs based on the dyes. The lower half in (a) shows the dark current densities of DSSCs.

DSSCs with an effective area of 0.16 cm² were fabricated using an electrolyte composed of 0.1 M LiI, 0.6 M DMPII, 0.05 M I₂, and 0.1 M GuSCN in ACN/MPN. The cell performance data under AM 1.5 illumination are collected in Table 1. The photocurrent–voltage (J - V) curves and the incident photon-to-current conversion efficiencies (IPCE) of the cells are shown in Figure 3. The IPCE values of the **BP** dyes are higher than that of **S1** by ~10–20%, which is consistent with the absorption spectra. The devices exhibited moderate to good power conversion efficiencies ranging from 5.33 to 5.95%. The adsorbed dye densities (**S1**, 4.34×10^{-7} ; **BP-1**, 4.01×10^{-7} ; **BP-2**, 4.54×10^{-7} ; **BP-3**, 3.86×10^{-7} mol cm⁻²) on the TiO₂ surface differed within 20%. Therefore, the higher J_{SC} of **BP-1** than that of **S1** can be ascribed to the better light harvesting of the former. The lower open-circuit voltage (V_{OC}) of **S1** than that of **BP** dyes may be due to the larger dark current density (Figure 3a) in the former. The highest J_{SC} and V_{OC}

- (4) (a) Thomas, K. R. J.; Lin, J. T.; Hsu, Y.-C.; Ho, K.-C. *Chem. Commun.* **2005**, 4098. (b) Chen, C.-H.; Hsu, Y.-C.; Chou, H.-H.; Thomas, K. R. J.; Lin, J. T.; Hsu, C.-P. *Chem.—Eur. J.* **2010**, *16*, 3184.
 (5) Lee, K.-M.; Hsu, Y.-C.; Ikegami, M.; Miyasaka, T.; Thomas, K. R. J.; Lin, J. T.; Ho, K.-C. *J. Power Sources*. **2011**, *196*, 2416.
 (6) Geiger, T.; Kuster, S.; Yum, J.-H.; Moon, S.-J.; Nazeeruddin, M. K.; Grätzel, M.; Nüesch, F. *Adv. Funct. Mater.* **2009**, *19*, 2720.
 (7) Pack, S.; Choi, H.; Lee, C.-W.; Kang, M.-S.; Song, K.; Nazeeruddin, M. K.; Ko, J. *J. Phys. Chem. C* **2010**, *114*, 14646.

Table 1. Optical, Redox, and DSSC Performance Parameters of the Dyes^a

dye	V_{OC} (V)	J_{SC} (mA cm ⁻²)	η (%)	FF	λ_{abs} ($\epsilon \times 10^{-4}$ M ⁻¹ cm ⁻¹) ^b nm	E_{ox} (ΔE_p) ^c mV
S1	0.59	10.94	4.22	0.66	418 (3.43)	570
					305 (2.45)	(153)
					443 (3.96)	509 (82)
BP-1	0.61	13.61	5.33	0.64	441 (4.03)	510
					308 (2.21)	(125)
BP-2	0.65	14.16	5.95	0.65	430 (3.65)	520
					335 (1.92)	(133)
BP-3	0.62	13.81	5.65	0.66	432 (3.68)	520
					345 (2.19)	(134)
N719	0.72	18.33	8.61	0.65		

^a Experiments were conducted using TiO₂ photoelectrodes with an approximately 20 μ m thickness and 0.16 cm² working area on the FTO (15 Ω /sq.) substrates. ^b Recorded in THF solutions at 298 K. ^c Recorded in THF solutions. $E_{ox} = 1/2(E_{pa} + E_{pc})$, $\Delta E_p = E_{pa} - E_{pc}$ where E_{pa} and E_{pc} are the anodic and cathodic peak potentials, respectively. The oxidation potential reported is adjusted to the potential of ferrocene which was used as an internal reference. The values in parentheses are the peak separation of cathodic and anodic waves. Scan rate: 100 mV s⁻¹.

of **BP-2** among all are likely due to the highest dye density and lowest dark current density of **BP-2** compared to other dyes.

BP-2 with the highest cell performance was subjected to cosensitization with SQ2 because the latter could compensate for the deficit of the former in the NIR region. DSSCs with the use of **BP-2** and SQ2 solutions of the same concentration in different volume ratios were fabricated. Figure 4a shows the absorption spectra of four TiO₂ films cast with various volume ratios of **BP-2**/SQ2.

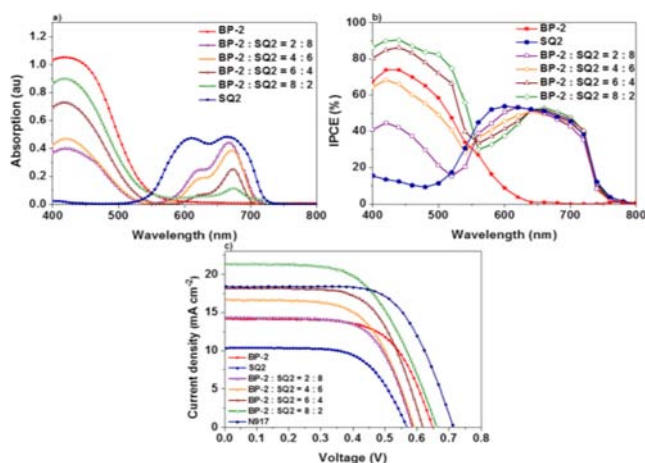


Figure 4. (a) Absorption spectra of **BP-2**/SQ2 coadsorbed on TiO₂ film (thickness ~2 μ m) in different volume ratios. (b) IPCE spectra of **BP-2**/SQ2 cosensitized cells. (c) J - V curves of **BP-2**/SQ2 cosensitized cells.

Strong absorption of the **BP-2** dye at wavelengths below 550 nm and absorption due to SQ2 in the red to NIR region

(600–800 nm) are evident. The IPCE spectra (Figure 4b) of **BP-2**/SQ2 cosensitized DSSCs cover a fairly broad range (400–750 nm). In accordance with the film spectra on TiO₂, high conversion efficiencies were noticed at 400–500 nm and 600–700 nm. The *J–V* curves for these **BP-2**/SQ2 cosensitized cells under AM 1.5 condition are shown in Figure 4c, and the performance parameters are collected in Table 2. The efficiency enhancement is in compliance with the increasing volume ratio of **BP-2**. It is intriguing that the *J*_{SC} values reach 18.15 and 21.33 mA cm⁻² at the **BP-2**/SQ2 ratio of 6:4 (v/v) and 8:2 (v/v), respectively. The highest efficiency was achieved with the lowest amount of SQ2. This outcome can be rationalized by two explanations: (1) the high molar extinction coefficient of SQ2 leads to absorption saturation at a relatively low concentration; (2) a low concentration of SQ2 avoids dye aggregation. To our knowledge, the efficiency of 8.14% (Table 2) is the highest among cosensitized DSSCs ever reported using metal-free sensitizers and Al₂O₃-free TiO₂.

Table 2. Performance Parameters of Cosensitized DSSCs^a

dye	V _{oc} (V)	<i>J</i> _{sc} (mA cm ⁻²)	η (%)	FF
BP-2	0.65	14.16	5.95	0.65
SQ2	0.57	10.33	3.78	0.64
BP-2 :SQ2 = 2:8	0.58	14.33	5.53	0.66
BP-2 :SQ2 = 4:6	0.59	16.67	6.09	0.62
BP-2 :SQ2 = 6:4	0.63	18.15	7.18	0.63
BP-2 :SQ2 = 8:2	0.66	21.33	8.14	0.58
N719	0.72	18.33	8.61	0.65

^aExperiments were conducted using TiO₂ photoelectrodes with an approximately 20 μm thickness and 0.16 cm² working area on the FTO (15 Ω/sq.) substrates.

The photocurrent estimated from integrating the product of the IPCE value at each wavelength and the photon flux density data in the AM 1.5 solar spectrum (100 mW/cm²)⁸ was ~16.5 mA/cm² for the **BP-2**:SQ2 (8:2) cell, which is smaller than the experimental value. This discrepancy may be attributed to the filtration of infrared radiation by a water filter in our light source during measurement, while the real sun spectrum⁸ covers the near-infrared portion.

The TiO₂ film adsorbed with cosensitizers **BP-2**/SQ2 in a ratio of 8:2 (v/v) was subjected to Auger electron spectroscopy (AES) for probing the dye distribution across the TiO₂ film. This technique is similar to the Electron Probe Micro-Analyzer (EPMA) method used by Park et al.⁹ and Ko^{3c} et al. for investigating the distribution of a specific element across the TiO₂ depth.

(8) Annual Book of ASTM Standards, ASTM International: West Con-shohocken, PA, 2003, Vol. 14.04, pp G159–98.

(9) Lee, K.; Park, S.-K.; Ko, M.-J.; Kim, K.; Park, N.-G. *Nat. Mater.* **2009**, *8*, 665.

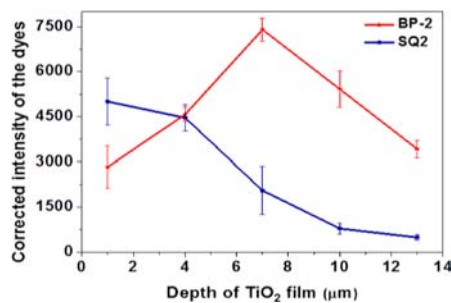


Figure 5. AES analysis showing the amounts of **BP-2** and SQ2 across the depth of the TiO₂ film at a 8:2 (v/v) ratio of **BP-2**/SQ2 cosensitized cells.

Figure 5 shows variation of the amounts (see experimental section) of **BP-2** and SQ2 along the TiO₂ film depth (0 μm is the interface of the scattering layer and the active layer of TiO₂). The amount of the SQ2 decreased with the increasing depth of TiO₂ film, while **BP-2** increased when the TiO₂ depth increased and reached maximum at ~7 μm, and then decreased. This can be rationalized by the more efficient penetration of **BP-2** into the TiO₂ film. We speculate that the higher molecular weight of SQ2 retards its penetration rate through the TiO₂ film. A similar concentration gradient was also found in Ko's cosensitized TiO₂ film via sequential adsorption of two different dyes.^{3c}

In summary, we have synthesized new arylamine sensitizers with a 9,10-dihydrophenanthrene entity in the conjugated spacer. The dyes have a very intense absorption ($\epsilon > 36\,500\text{ M}^{-1}\text{ cm}^{-1}$) at ~430 nm. High performance cosensitized DSSCs with a conversion efficiency up to 8.14% can be achieved. This represents the highest cosensitized DSSC using all metal-free sensitizers and without the use of Al₂O₃-coated TiO₂. Moreover, cosensitization from the mixture of different dyes simplifies the cell fabrication process. The concentration distribution found in this study demonstrates that the strategy can be extended to other systems if dyes are appropriately chosen.

Acknowledgment. We acknowledge the support of the Academia Sinica (AC) and NSC (Taiwan), and the Instrumental Center of Institute of Chemistry (AC).

Supporting Information Available. Synthetic procedures and characterization for new compounds. This material is available free of charge via the Internet at <http://pubs.acs.org>.

The authors declare no competing financial interest.